Optimal Experiment Design for the estimation of building wall material thermal properties

Ainagul Jumabekova, Julien Berger

Optimal Experiment Design for the estimation of building wall material thermal properties

Ainagul Jumabekova[1]*, **Julien Berger**[1]

[1] Laboratoire des Sciences de l'Ingénieur pour l'Environnement (LaSIE), UMR 7356 CNRS, La Rochelle Université, CNRS, 17000, La Rochelle, France

E-mail: ainagul.jumabekova@univ-lr.fr, ORCiD: 0000-0001-5554-4249

Abstract. The estimation of wall thermal properties through an inverse problem procedure enables to increase the reliability of the model predictions for building energy efficiency. Nevertheless, it requires to define an experimental campaign to obtain on-site observations for existing buildings. The design of experiments enables to search for the optimal measurement plan that ensure the highest precision of the parameter estimation. For on-site measurement in buildings, it seeks an answer to several questions such as number and position of sensors, period and duration of the experimental campaign. In this article, the Optimal Experiment Design (OED) methodology is applied for a multi-layer building wall to resolve the aforementioned issues.

1. Introduction

One of the current environmental challenges is to reduce carbon emissions. Since the building sector is responsible for approximately one-third of global energy-related carbon emissions [1, 2], it is important to optimize the energy efficiency of the building stock in the future. One approach is to apply a building retrofitting procedure on existing buildings. Before starting the procedure engineers perform energy performance simulations to predict whether the implemented measures are efficient. However, several studies have found a discrepancy in the energy performance of real buildings compared to the simulated values, so-called as "performance gap" [3]. This gap arises from properties of building materials, as they differ from initial values due to building degradation and operation, exposed weather conditions, etc. Therefore, one should determine and evaluate current material properties of a wall.

The quality of the parameter estimation strongly depends on the quality of the experimental data used for the parameter identification. Pronzato in [4] highlights the relation between the experiment design and the precision of the retrieved parameters. The design of experiments enables to search for the optimal measurement plan that ensure the highest precision of the parameter estimation. For on-site measurement in buildings, the design of experiments seeks in answering to the following questions, synthesized in Figure 1. How many sensors are required? One should take into account that a higher number of sensors ensure a higher accuracy of estimates, however, it will raise the cost and the destructiveness of the experiment. What sensor position X in the wall? When to perform experimental campaign, in winter or in summer period? How long the measurements should be held? In other words, what is the sequence Ω_t^{oed} to carry the experiments in the wall? Since measurements are taken in the existing buildings, their

duration should be limited to avoid disturbance of the residents. It also avoids overall cost of the parameter estimation procedure. Finally, with on-site measurements, the boundary conditions cannot be controlled since they are imposed by the weather conditions forcing transient states in the wall.

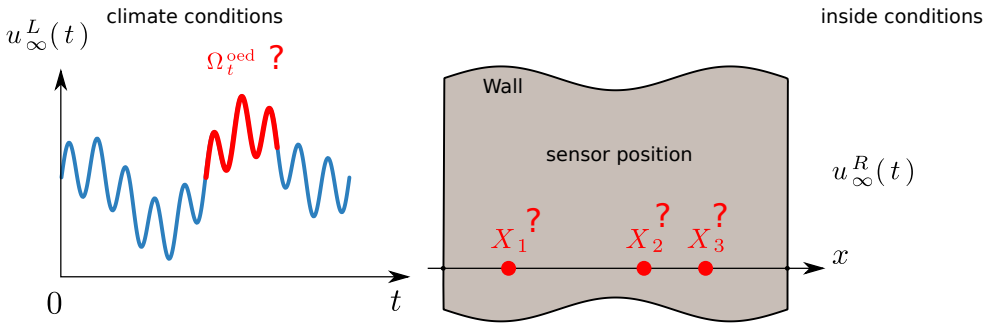

Figure 1: Issues to define the optimal experiment design for parameter estimation of building wall thermophysical properties.

The Optimal Experiment Design (OED) methodology enables to answer those questions [5, 6, 7]. For example, an optimal sensor location and heating period were identified to estimate thermal conductivity and volumetric heat capacity of composite materials [8]. Furthermore, Karalashvili et al. [9] searched OED for the estimation of the transport coefficient in the convection-diffusion equation. Artyukhin and Budnik [10] inspected the optimal sensor location and their quantity in the inverse heat conduction boundary problem. Various scalar measures of performance, or so-called optimum criteria, based on the Fisher information matrix (FIM) associated with the parameters to be identified, are proposed [11]. D-criterion and E-criterion were used to determine the optimal length of an experiment to estimate the effective thermal conductivity during the coupled conduction and free convection heat transfer in a porous medium [12]. More recently, in [13], the optimal heating period and the duration of the experiment were investigated for a three-layer experimental set-up, where a thin heater is placed between two identical samples. A number of articles calculate an optimal criterion on mass transfer in a porous building material [14, 15]. Several studies [16, 17, 18] use the D-optimum criterion to design the experiment with respect to the magnitude of the applied heat flux, heating and final experimental times, as well as the number and locations of sensors for parameter estimation for heat and mass transfer in capillary porous media. The aforementioned works consider experiments in laboratory setup for a specimen, considering heat and/or mass transfer problems under controlled conditions. However, it is important to enlarge the implementation of OED to building physics, where experiments are designed rather empirically [19, 20]. Thus, the objective of this paper is to introduce the application of the OED methodology for an experiment at wall scale, to propose a theoretical criterion to evaluate the accuracy of experiment. For this, a base case scenario of heat conduction transfer through a wall is considered. Then, optimal sensor positions within the wall and a period, when to start the experiment, are found.

The article is organized in the following way. At first, the physical model is defined together with its sensitivity equations. Then, the numerical solution of the sensitivity coefficients using the Dufort–Frankel numerical scheme is introduced. Next, the concept of an optimal experiment design is demonstrated. Finally, the case study of a building wall is described, and an optimal measurement plan is found.

2. Methodology

2.1. Physical model

First, a mathematical formulation of heat transfer through a multi-layer wall is presented. The

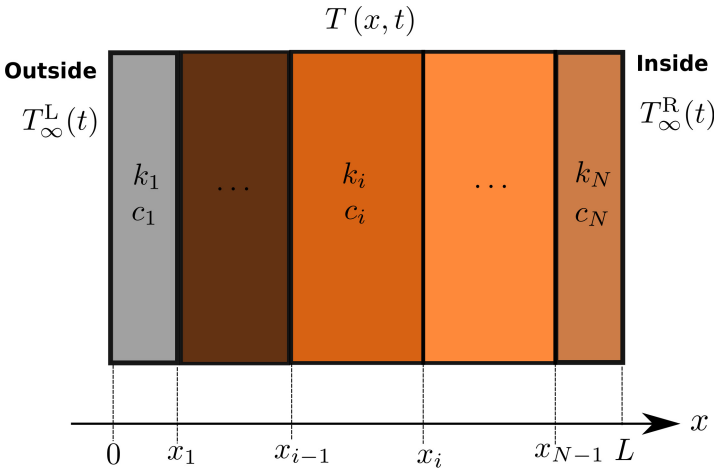

Figure 2: Illustration of a wall domain.

physical problem considers one–dimensional heat conduction transfer through a building wall. The wall is composed of N layers, each layer differs from the other by its thermal properties and thickness as shown in Figure 2. The temperature $T\,[\,\mathsf{K}\,]$ in the wall is defined on the domains $\Omega_x = \{\, x \,|\, x \in [\,0\,, L\,]\,\}$ and $\Omega_t = \{\, t \,|\, t \in [\,0\,, \tau_{\max}\,]\,\}$, where $L\,[\,\mathsf{m}\,]$ is the length of the wall and $\tau_{\max}\,[\,\mathsf{s}\,]$ is the duration of the experiment:

$$T : [\,0\,, L\,] \times [\,0\,, \tau_{\max}\,] \longrightarrow \mathbb{R}\,.$$

The mathematical formulation of the heat transfer process is given below [21]:

$$c\,\frac{\partial T}{\partial t} = \frac{\partial}{\partial x}\left(k\,\frac{\partial T}{\partial x}\right), \tag{1}$$

where $c\,[\,\mathsf{J}\cdot\mathsf{K}^{-1}\cdot\mathsf{m}^{-3}\,]$ is the volumetric heat capacity, or $c = \rho\cdot c_p$, corresponding to the product between the material density $\rho\,[\,\mathsf{kg}\cdot\mathsf{m}^{-3}\,]$ and the specific heat $c_p\,[\,\mathsf{J}\cdot\mathsf{kg}^{-1}\cdot\mathsf{K}^{-1}\,]$, and $k\,[\,\mathsf{W}\cdot\mathsf{m}^{-1}\cdot\mathsf{K}^{-1}\,]$ is the thermal conductivity.
Material thermal properties depend on the space coordinate, which means that the value of the property of each layer is taken into account:

$$c : x \longmapsto \sum_{i=1}^{N} c_i \cdot \varphi_i(x)\,,$$

where $\{\,\varphi_i(x)\,\}_{\,i\,=\,1,\ldots,N}$ are piecewise functions and can be written as:

$$\varphi_i(x) = \begin{cases} 1\,, & x_{i-1} \leqslant x \leqslant x_i\,, \quad i = 1,\ldots,N\,, \\ 0\,, & \text{otherwise}\,, \end{cases}$$

where x_{i-1} and x_i are the left and right interfaces of layer i, respectively. A similar definition is assumed for the thermal conductivity k:

$$k : x \longmapsto \sum_{i=1}^{N} k_i \cdot \varphi_i(x)\,.$$

Therefore, equation (1) becomes:

$$\sum_{i=1}^{N} c_i \, \varphi_i(x) \, \frac{\partial T}{\partial t} \;=\; \frac{\partial}{\partial x} \left(\sum_{i=1}^{N} k_i \, \varphi_i(x) \, \frac{\partial T}{\partial x} \right). \tag{2}$$

The following boundary conditions are defined, using the obtained inside and outside surface temperatures measurements:

$$T \;= T_{\infty}^{L}(t), \qquad x \;=\; 0, \tag{3}$$

$$T \;= T_{\infty}^{R}(t), \qquad x \;=\; L. \tag{4}$$

At the initial state the temperature is given as:

$$T(x, t \;=\; 0) \;=\; T_0(x) \tag{5}$$

2.2. Dimensionless formulation

In order to minimize the round–off numerical errors and to analyze the model behaviour regardless the used units for variables, it is essential to obtain a dimensionless formulation of the problem [22, 23]. To convert equation (1) the following dimensionless variables are introduced:

$$x^{\star} \;=\; \frac{x}{L}, \qquad\qquad u \;=\; \frac{T \;-\; T_{\mathrm{ref}}}{\Delta T_{\mathrm{ref}}}, \qquad\qquad t^{\star} \;=\; \frac{t}{t_{\mathrm{ref}}},$$

as well as dimensionless thermal properties functions by:

$$k^{\star} \stackrel{\mathrm{def}}{:=} \frac{k}{k_{\mathrm{ref}}}, \qquad\qquad c^{\star} \stackrel{\mathrm{def}}{:=} \frac{c}{c_{\mathrm{ref}}}.$$

where subscripts **ref** relate for a characteristic reference value, and superscript $\star$ for dimensionless parameters.
Thus, equation (1) transforms to:

$$c^{\star} \, \frac{\partial u}{\partial t^{\star}} \;=\; \mathrm{Fo} \, \frac{\partial}{\partial x} \left(k^{\star} \, \frac{\partial u}{\partial x^{\star}} \right), \tag{6}$$

where $\mathrm{Fo} \;=\; \dfrac{t_{\mathrm{ref}} \, k_{\mathrm{ref}}}{L^2 \, c_{\mathrm{ref}}}$ is FOURIER number.

The DIRICHLET–type boundary conditions are converted to:

$$u \;= u_{\mathrm{L}}(t^{\star}), \qquad x^{\star} \;=\; 0, \qquad \text{where} \qquad u_{\mathrm{L}} \;=\; \frac{T_{\infty}^{L} \;-\; T_{\mathrm{ref}}}{\Delta T_{\mathrm{ref}}}, \tag{7}$$

$$u \;= u_{\mathrm{R}}(t^{\star}), \qquad x^{\star} \;=\; 1, \qquad \text{where} \qquad u_{\mathrm{R}} \;=\; \frac{T_{\infty}^{R} \;-\; T_{\mathrm{ref}}}{\Delta T_{\mathrm{ref}}}. \tag{8}$$

Furthermore, the initial condition is transformed to:

$$u \;=\; u_0(x^{\star}), \qquad \text{where} \qquad u_0 \;=\; \frac{T_0 \;-\; T_{\mathrm{ref}}}{\Delta T_{\mathrm{ref}}}. \tag{9}$$

Further in the article, for the sake of the clarity the superscript $\star$ is omitted, and all results are presented in dimensionless form unless stated otherwise.

2.3. Sensitivity equations

One may consider solution u of Eq. (6) as a model output. The solution u may be declared as a function of $(x, t, \boldsymbol{p})$, where $\boldsymbol{p}$ is a vector of model parameters. In our case one may formulate is as follows:

$$u : (x, t, \boldsymbol{p}) \longmapsto u(x, t, \boldsymbol{p}),$$
$$\text{where } \boldsymbol{p} \in \{k_i, c_i\}, \forall\, i = 1 \ldots N$$

Furthermore, new variables X_{p_i} or sensitivity coefficients are introduced, which quantify the model output sensitivity to the parameter p_i.

$$X_{p_i} \stackrel{\text{def}}{:=} \frac{\partial u}{\partial p_i}.$$

The sensitivity coefficients are obtained as a solution of a differential equation or sensitivity equation, which is a result of partial differentiation of the model equation. For the sake of simplicity, one may find sensitivity equations for the thermal conductivity of the first layer. The following new variable is presented:

$$X_{k_1} \stackrel{\text{def}}{:=} \frac{\partial u}{\partial k_1}.$$

Next, one may differentiate Eq. (6) with respect to parameter k_1 and obtain the differential equation for X_{k_1}:

$$\frac{\partial X_{k_1}}{\partial t} = \frac{\mathrm{Fo}}{c} \frac{\partial}{\partial x} \left(\frac{\partial k}{\partial k_1} \frac{\partial u}{\partial x} + k \frac{\partial X_{k_1}}{\partial x} \right) \tag{10}$$

2.4. Numerical solution

First, the space Ω_x and time Ω_t intervals are discretized uniformly, with the parameters Δx and Δt, respectively. The discrete values of function $u(x,t)$ are defined as $u_j^n \stackrel{\text{def}}{:=} u(x_j, t_n)$, where $j \in \{1, \ldots, N_x\}$ and $n \in \{1, \ldots, N_t\}$.

Numerical solution of the Eq. (6) is obtained using Dufort–Frankel scheme [24]. This numerical scheme allows to compute explicitly the solution at each time step, and it has the unconditionally stable property. The numerical scheme is expressed as the following explicit formulation:

$$u_j^{n+1} = \nu_1 u_{j+1}^n + \nu_2 u_{j-1}^n + \nu_3 u_j^{n-1}, \tag{11}$$

where

$$\nu_1 = \frac{\lambda_1}{\lambda_0 + \lambda_3}, \qquad \nu_2 = \frac{\lambda_2}{\lambda_0 + \lambda_3}, \qquad \nu_3 = \frac{\lambda_0 - \lambda_3}{\lambda_0 + \lambda_3},$$

and

$$\lambda_0 = 1, \qquad \lambda_1 = \frac{2\Delta t}{\Delta x^2} \frac{\mathrm{Fo}}{c_j} k_{j+\frac{1}{2}} \qquad \lambda_2 = \frac{2\Delta t}{\Delta x^2} \frac{\mathrm{Fo}}{c_j} k_{j-\frac{1}{2}},$$
$$k_{j\pm\frac{1}{2}} = k\left(\frac{x_j + x_{j\pm1}}{2}\right), \quad \lambda_3 = \frac{\Delta t}{\Delta x^2} \frac{\mathrm{Fo}}{c_j} \left(k_{j+\frac{1}{2}} + k_{j-\frac{1}{2}}\right).$$

In order to calculate the sensitivity coefficients efficiently, the direct differentiation of the numerical scheme Eq. (11) with respect to the required parameter is used.

One may obtain the numerical scheme for computing sensitivity coefficient X_{k_1} of the model output $u(x,t)$ with a respect to a parameter k_1, by partially differentiation of each term of Eq. (11), which is presented below:

$$X^{n+1}_{k_1 j} = \nu_1 X^{n}_{k_1 j+1} + \nu_2 X^{n}_{k_1 j-1} + \nu_3 X^{n-1}_{k_1 j} + \frac{\partial \nu_1}{\partial k_1} u^{n}_{j+1} + \frac{\partial \nu_2}{\partial k_1} u^{n}_{j-1} + \frac{\partial \nu_3}{\partial k_1} u^{n-1}_{j} .$$

2.5. Optimal Experiment Design

To search for an optimal experiment design (OED), first, a measurement plan is defined. It includes experiment conditions, that can be modified during the experimental campaign. First, since the measurements are taken using thermocouples sensors, the questions, where within the wall to install the sensors, and how many sensors are required to use, arise. Moreover, since the measurements are performed on-site, weather conditions and seasonal temperature variation have a great impact on the success of the experimental campaign. Therefore, it is important to determine when to obtain the measurements, and how long the experimental campaign should be held. Consequently, the following measurement plan is presented:

$$\pi = \{ t_{\text{ini}}, \delta\tau, N_{\text{s}}, \chi_{\text{s}} \}, \tag{12}$$

where t_{ini} and $\delta\tau$ are the starting day and duration of the experimental campaign respectively, χ_{s} is sensors location, and N_{s} is the number of sensors. The measurement plan considers the whole interval of the space domain Ω_x for the sensor position χ_{s}. In addition, the reduced experimental campaign sequence is defined as follows:

$$\Omega_t^{\text{oed}} = [t_{\text{ini}}, t_{\text{ini}} + \delta\tau],$$

while the following condition $\Omega_t^{\text{oed}} \subset \Omega_t$ is respected.

The optimal measurement plan is determined by maximization of the D-optimum criterion [5, 11], which describes the accuracy of the estimated parameters. Thus, OED is formulated as follows:

$$\hat{\pi} = \underset{\pi}{\operatorname{argmax}} \Psi , \tag{13}$$

where Ψ is the determinant of the Fisher matrix $\widetilde{\mathrm{F}}(\pi)$

$$\Psi = \det \widetilde{\mathrm{F}}(\pi). \tag{14}$$

The elements of the matrix $\widetilde{\mathrm{F}}(\pi)$ represent the average value of the parameters sensitivity coefficients during the measurement plan π and are defined according to [5]:

$$\widetilde{\mathrm{F}}(\pi) = \left[\widetilde{\mathrm{F}}_{ij} \right], \qquad \forall (i,j) \in \{1, ..., N_p\}, \tag{15}$$

$$\widetilde{\mathrm{F}}_{ij} = \frac{1}{\delta\tau} \sum_{r=1}^{N_{\text{s}}} \frac{1}{\sigma^2} \int_{\Omega_t^{\text{oed}}} X_{p_i} X_{p_j} \, \mathrm{dt}, \tag{16}$$

where X_{p_i} is the sensitivity coefficient of the solution related to the parameter p_i, σ is the measurement uncertainty, N_p is the number of parameters, and N_{s} is the total number of measurements. In addition, the normalized criterion value is denoted as a ratio between the determinant of the Fisher matrix for this particular measurement plan and the found maximum value:

$$\widehat{\Psi} = \frac{\Psi}{\max\limits_{\pi} \Psi} .$$

3. Case Study

Aim of this section is to demonstrate how to find an optimal measurement plan, which allows one to estimate the thermal conductivity with high accuracy. One may recall questions, which have been raised in the context of on-site experimental set-up. Where inside the wall the sensors are to be installed? How many sensors are required to use? When should the experiment start? How long should it last? First, an one–story house with a single room is chosen and simulated in EnergyPlus software [25].

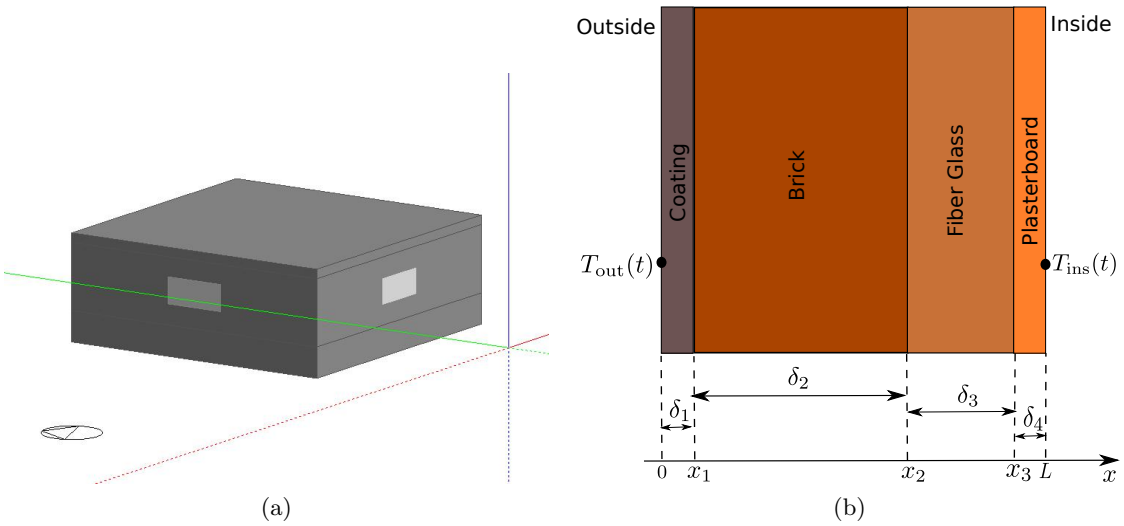

Figure 3: Illustration of the modeled house *(a)* and the wall construction *(b)*.

Figure 3a shows the geometry of the modeled house. It consists of single room and three zones: crawl space, living space, and roof space. The envelope has several types of composition. First, the vertical walls are composed of a 5 cm fiber glass insulation and a 25 cm layer of brick as presented in Figure 3b. Each wall has a window, all windows are double-glazed and filled with argon. Next, the roof is constructed of clay tiles and layer of thermal insulation material. The ground floor consists of concrete slab and thermal insulation material. Details about the composition materials are presented further. The *a priori* wall material properties and its layer thickness are presented in Table 1. These properties are used to construct the direct model and to simulate the building energy performance in the EnergyPlus software. The material properties are obtained from [26].

Table 1: The *a priori* properties of the wall layers.

Material	Thermal conductivity $k^\circ\ [\mathsf{W}\cdot\mathsf{K}^{-1}\cdot\mathsf{m}^{-1}]$	Specific heat $c_{\text{p}}^\circ\ [\mathsf{J}\cdot\mathsf{K}^{-1}\cdot\mathsf{kg}^{-1}]$	Density $\rho^\circ\ [\mathsf{kg}\cdot\mathsf{m}^{-3}]$	Thickness $\delta\ [\mathsf{cm}]$
Coating	1.15	850	2000	1
Brick	1.0	920	1800	25
Fiber Glass	0.033	840	43.4	5
Plasterboard	0.25	1000	820	2.5

Next, to answer aforementioned questions about experimental campaign, the following measurement plan is considered:

$$\pi \;=\; \{\, t_{\text{ini}}\,,\, \delta\tau\,,\, N_{\text{s}}\,,\, \chi_{\text{s}}\,\}\,, \tag{17}$$

where t_{ini} and $\delta\tau$ are the starting day and duration of the experimental campaign respectively, χ_{s} is sensors location, and N_{s} is the number of sensors. In addition, the reduced experimental campaign sequence is defined as follows:

$$\Omega_t^{\text{oed}} \;=\; [\, t_{\text{ini}}\,,\, t_{\text{ini}} \;+\; \delta\tau\,]\,.$$

A choice of the duration of the experiment $\delta\tau$ is discussed first. Previously, an empirical study is conducted in [27]. The findings of the article suggest to carry out experiment at least 3 days. Moreover, as mentioned earlier, occupants should be not disturbed during long period. Also, as demonstrated in [28], 3 days is a good compromise between the computational time of the parameter estimation problem and the maximum value of D-optimum criterion. Thus, the measurement plan considers $\delta\tau \;=\; 3$ days as an optimal number of days to perform experimental campaign. As a result, during one year of observations 363 possible periods should be assessed. It can be formulated as:

$$\delta\tau \;=\; 3\,\text{days}\,, \quad t_{\text{ini}} \;\in\; [\,1\,,363\,] \quad [\,\text{day(s)}\,]\,, \quad \Omega_t^{\text{oed}} \;=\; [\,t_{\text{ini}}\,,\, t_{\text{ini}} \;+\; 3\,]\,, \quad N_{\delta\tau} \;=\; 363\,.$$

Next issue is to determine temperature sensors quantity and its position within the wall. The number of sensors is discussed first. In this case study two sensors positions are determined in brick and insulation layer respectively. These two layers are remain in case of retrofitting procedure. Moreover, from a practical point of view, it is easier to install two sensors inside the wall, since it less perturbs the physical process of heat transfer within the wall. For this reason, the study is conducted using $N_{\text{s}} \;=\; 2$. Figure 4 illustrates the experimental design. One may

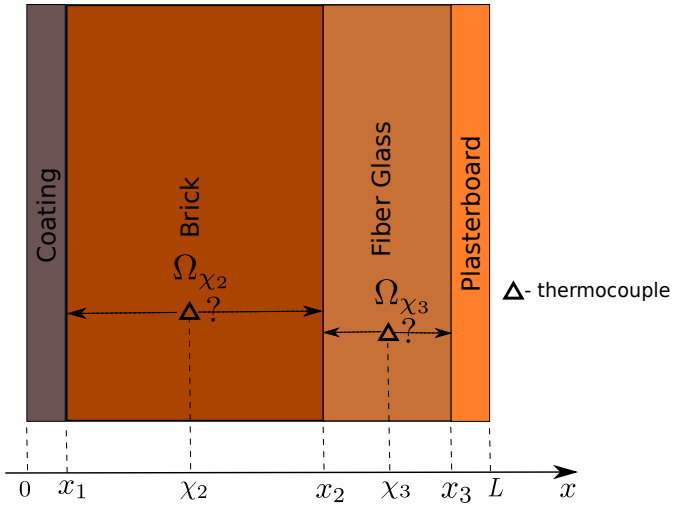

Figure 4: Possible positions of 2 sensors within the brick and insulation layers.

use the following expressions to formulate the problem:

$$\chi_{\text{s}} \;=\{\,\chi_2\,,\chi_3\,\}\,, \qquad \chi_2 \;\in\; [\,x_1\,,\,x_2\,]\,, \qquad \chi_3 \;\in\; [\,x_2\,,\,x_3\,]\,.$$

In other words, the first sensor position, noted as χ_2, is within the brick layer. While the second sensor location χ_3 is inside the insulation layer. Thus, the measurement plan is searched as follows:

$$\pi \;=\; \{\, t_{\text{ini}}\,,\, \chi_2\,,\, \chi_3\,\}\,.$$

3.1. Results and Discussion

Before starting to calculate the D-optimum criterion, it is important to obtain possible sensors positions within corresponding layer. For this, each layer is discretized, and potential sensor positions is retrieved. It can be written as:

$$\Omega_{\Delta\chi_2} = \{\chi_2^j : \chi_2^{j+1} - \chi_2^j = \Delta\chi_2\}, \qquad \chi_2^j \in [x_1, x_2], \qquad j = 1, \ldots, N_{s2},$$
$$\Omega_{\Delta\chi_3} = \{\chi_3^j : \chi_3^{j+1} - \chi_3^j = \Delta\chi_3\}, \qquad \chi_3^j \in [x_2, x_3], \qquad j = 1, \ldots, N_{s3}.$$

For this case study, the following values are chosen. The number of potential sensors locations inside the brick layer is set as $N_{s2} = 15$, which corresponds to the discretization step equal to $\Delta\chi_2 = 1,67$ cm. This value shows the distance between two possible sensors locations. The quantity of possible thermocouples inside the insulation layer is set as $N_{s3} = 8$, and the step is $\Delta\chi_3 = 0,625$ cm. This value corresponds to the size of the temperature sensor, which is equal to 0.5 cm. It can be noted, that within the insulation layer more profound discretization is used. It is due to the fact that insulation layer has larger impact on the thermal loads than the brick. Thus, the position of the second sensor should be determined precisely. Now, the measurement plan includes $N_{\delta\tau} \times N_{s2} \times N_{s3}$ number of experiment designs. Using it, the D-optimum criterion Ψ is computed for each design, and maximum is calculated.

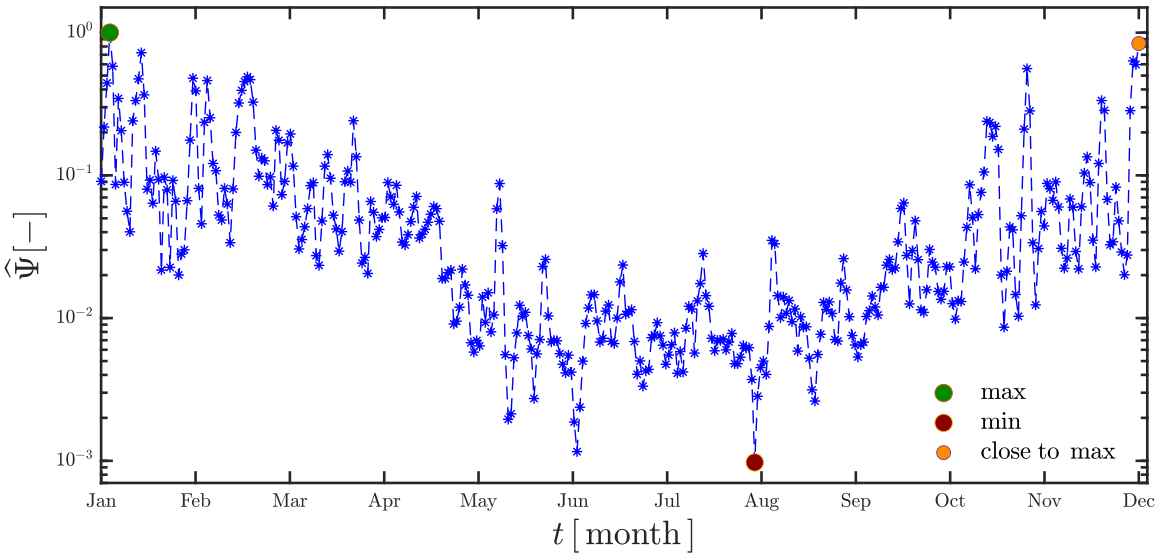

Figure 5: Values of criterion $\widehat{\Psi}$ according the starting day of the experimental campaign.

First, the optimal starting day is found. Figure 5 displays values of the relative D–optimum criterion $\widehat{\Psi}$ depending on the selection of the starting day of experimental campaign. It demonstrates how the relative criterion $\widehat{\Psi}$ composed of 363 values varies during the whole year of the experimental campaign. It can be noted that the high values of the criterion take place during the winter season, providing better accuracy for the parameter estimation problem. The lower values are related to the summer season. It corresponds to the fact that, in general, the amplitudes of the sensitivity coefficients during the winter period are higher compared to the summer period. These results are illustrated in Figure 6. Figures 6a and 6b display the variation of the sensitivity coefficients during three days in January for the two sensors in brick and insulation layers. In addition, Figures 6c and 6d present the same information during a three day period in June corresponding to the period of the experimental design with small values of D-criterion. As a result, the model is more sensitive to the parameters during the

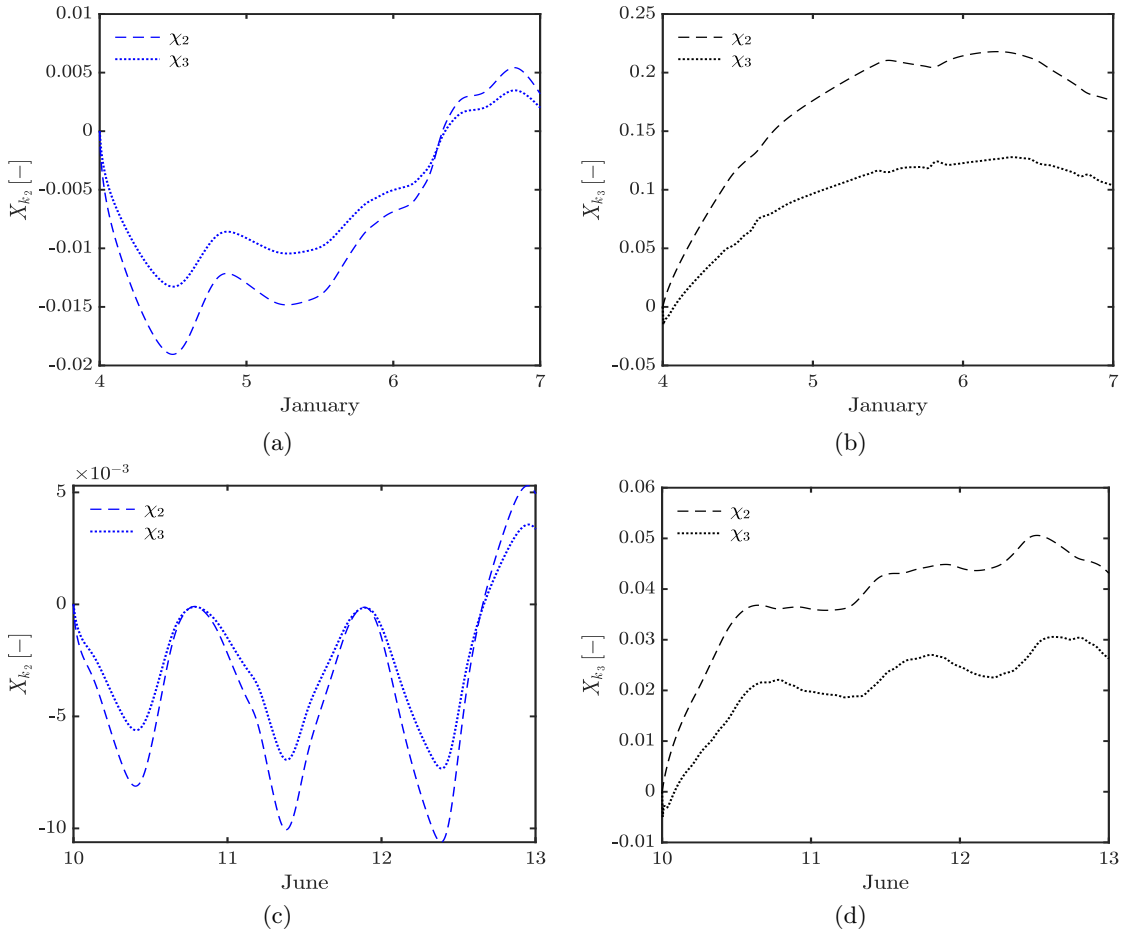

Figure 6: Variation of the sensitivity functions of the parameters *(a),(c)* k_2 and *(b),(d)* k_3 during winter and summer period.

cold season. In conclusion, one may note that the criterion reaches its maximum on January 4th. Thus, observations should be recorded from this date. Moreover, as shown in Figure 5, the second measurement plan is possible with the starting day on December 27th. From a practical point of view, it is important to start the experimental set-up before the chosen date, at least 3 days before. This period of time is used to install and calibrate sensors, also to stabilize temperature perturbations within the wall.

Next, the positions of the sensors are obtained. Figure 7 demonstrates how the relative D–optimum criterion varies according to sensor position in the brick and insulation layers. The maximum takes place near the interface between two layers. Therefore, sensors should be placed in these positions to ensure the best accuracy of observations. Since installing sensor is a procedure with uncertainty, an optimal sensor position is widened by 10% of the maximum value. These positions are shown in grey area in Figures 7a and 7b. It means that sensors can be placed within this area; nevertheless, a high level of accuracy for estimation is maintained. Therefore, an optimal measurement plan is obtained and expressed as:

$$\widehat{\pi} \;=\; \{\, \widehat{t_{\text{ini}}}\,,\, \widehat{\chi_2}\,,\, \widehat{\chi_3}\,\}\,,$$

where $\widehat{t_{\text{ini}}}$ is January 4th, $\widehat{\chi_2} \;=\; 24.45 \;\pm\; 2.4$ cm, and $\widehat{\chi_3} \;=\; 26.1 \;\pm\; 0.6$ cm. Using this information, an engineer obtain observations, which are useful to attain the highest accuracy

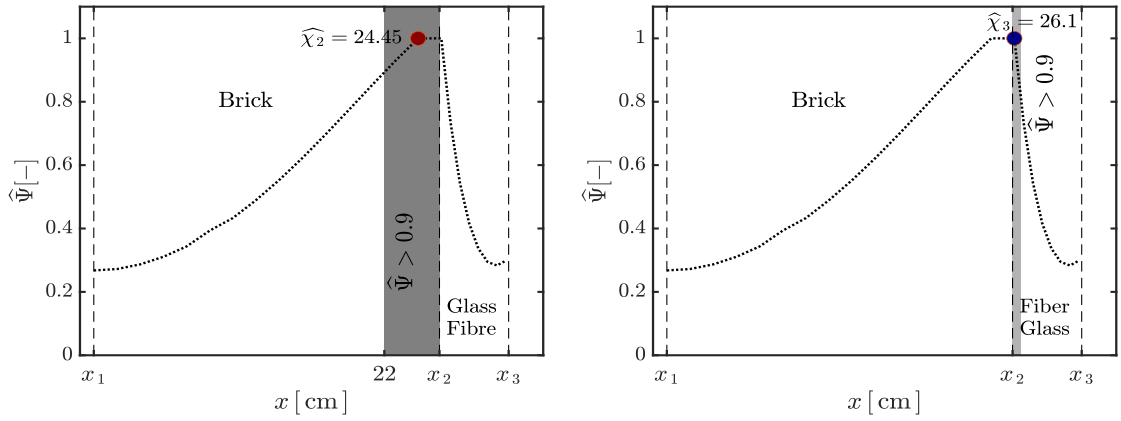

Figure 7: The optimal sensor position within *(a)* brick and *(b)* insulation layers.

for parameter estimation problem.

Furthermore, to verify the sensitivity analysis conclusions, the continuous derivative-based approach can be used to explore the sensitivity of continuous model output due to changes in the parameters. First, one may evaluate how the heat flux fluctuates according to the variation of the thermal conductivity and the volumetric heat capacity of the brick and insulation layers. Both thermal parameters vary by $\pm 50\%$ of their *a priori* values, presented in Table 1. Subsequently, the heat flux on the interior surface is approximated through the TAYLOR series expansion using the calculated sensitivity coefficients. Figures 8, 9 show the variation of the heat flux on the interior wall surface during the last three days in December. One may assess how the heat flux is affected by the thermal conductivity parameter; moreover, the thermal conductivity has a greater influence on the heat flux than the heat capacity. Additionally, it can be noted, that the heat capacity of the brick impacts the heat flux contrary to the heat capacity of the insulation layer.

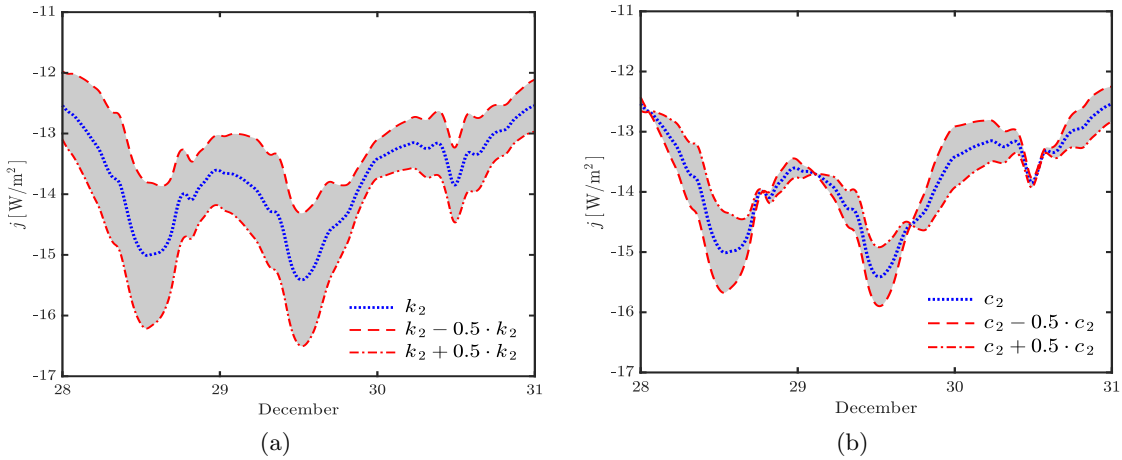

Figure 8: Variation in heat flux according to the thermal conductivity and volumetric heat capacity of the brick layer using TAYLOR series expansion.

Several remarks should be noted. First, the study considers embedded temperature sensors inside a wall due its high accuracy. One may notice that this experimental setup is destructive, and,

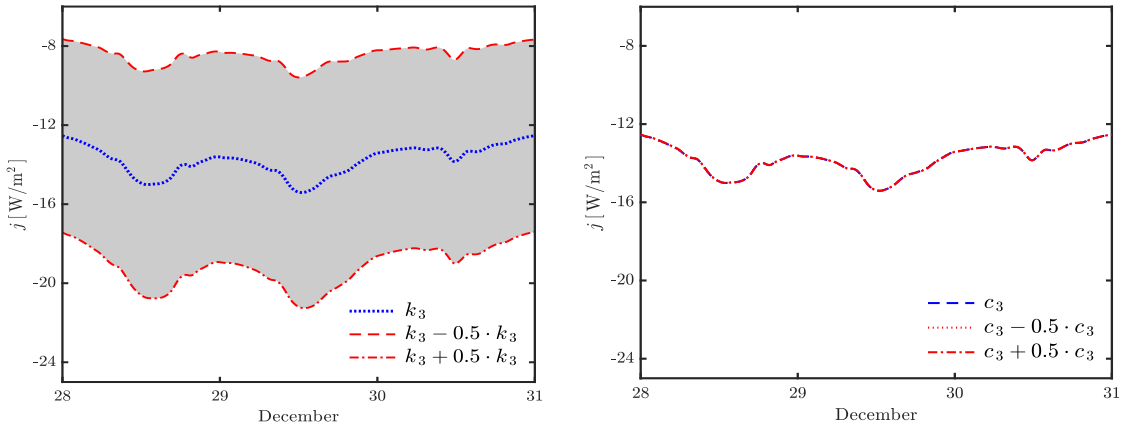

(a) (b)

Figure 9: Variation in heat flux according to the thermal conductivity and volumetric heat capacity of the insulation layer using TAYLOR series expansion.

thus, the implementation may be difficult. To tackle this issue a semi-destructive approach may be applied by using heat flux sensors. Moreover, temperature measurements may be recorder using an infrared camera. Since the objective of this article is to introduce the OED methodology at wall scale, one may apply it to compare optimal criteria using different measurement devices and select an appropriate experimental design. Next, the proposed framework is applied using simulated data. It is important to validate the methodology *in situ* on existing building, which should be investigated further. However, the proposed methodology may be considered at the initial stage of retrofitting procedure. Engineers may utilize synthetic data, provided by building simulation software, and obtain preliminary data of experimental design, such as starting date and period as well as optimal position of various available sensors. As mentioned earlier, similar results of optimal criterion were obtained for a wall of an old historical building [27]. Using identified optimal period of measurements, the thermal conductivity of the multi-layer wall were estimated with high precision.

4. Conclusion

The building sector is one of the main contributors to the total energy consumption worldwide. To maintain the building energy efficiency and improve the quality of the retrofitting solution one may employ a calibration of the building simulation model. Thus, values of thermophysical properties of the materials used to construct the building walls are inferred by the so-called inverse technique. One of the challenges of the parameter estimation approach is to obtain experimental observations, which ensure the best accuracy of estimates. The OED methodology enable to define the experimental campaign, performing which one may determine the required properties with the highest accuracy. In this paper, a building envelope, typical in France, is simulated in the EnergyPlus software. Using the generated data and the OED, an engineer may find an optimal measurement plan before starting the actual campaign. To demonstrate it, two optimal sensors positions within wall layers are found. Additionally, the optimal starting day of the on-site measurements during one year of observations is determined. Therefore, the OED theory provides a useful information about the experimental campaign before its initiation. Moreover, the obtained measurements increase the accuracy of the parameter estimation results.

References

[1] Dulac J, Abergel T and Delmastro C 2019 Tracking buildings Tech. rep. International Energy Agency, Paris
[2] Administration U E I 2015 *Annual Energy Outlook 2015, with Projections to 2040* (Washington: EIA)
[3] Marshall A, Fitton R, Swan W, Farmer D, Johnston D, Benjaber M and Ji Y 2017 *Energy and Buildings* **150** 307–317
[4] Pronzato L 2008 *Automatica* **44** 303 – 325 ISSN 0005-1098
[5] Beck J and Arnold K 1977 *Parameter estimation in engineering and science* (Wiley) ISBN 9780471061182
[6] Emery A F and Nenarokomov A V 1998 *Measurement Science and Technology* **9** 864–876
[7] Raynaud M 1999 *High Temperatures-high Pressures* **31** 1–15
[8] Taktak R, Beck J and Scott E 1993 *International Journal of Heat and Mass Transfer* **36** 2977–2986 ISSN 0017-9310
[9] Karalashvili M, Marquardt W and Mhamdi A 2015 *Computers and Chemical Engineering* **80** 101 – 113 ISSN 0098-1354
[10] Artyukhin E A and Budnik S A 1985 *Journal of engineering physics* **49** 1453–1458
[11] Ucinski D 2004 *Optimal Measurement Methods for Distributed Parameter System Identification* (New York: CRC Press) ISBN 978-0849323133
[12] Sami Z, Albouchi F, Mzali F, Jemni A and Ben Nasrallah S 2009 *Journal of Porous Media* **12** 573–583
[13] D'Alessandro G and de Monte F 2019 *International Journal of Heat and Mass Transfer* **134** 1268 – 1282 ISSN 0017-9310
[14] Berger J, Dutykh D and Mendes N 2017 *Experimental Thermal and Fluid Science* **81** 109 – 122 ISSN 0894-1777
[15] Berger J, Busser T, Dutykh D and Mendes N 2019 *Inverse Problems in Science and Engineering* **27** 735–772
[16] Dantas L, Orlande H, Cotta R and Lobo P 2000 Parameter estimation in moist capillary porous media by using temperature measurements *Inverse Problems in Engineering Mechanics II* ed Tanaka M and Dulikravich G (Oxford: Elsevier Science Ltd) pp 53 – 62
[17] Dantas L, Orlande H and Cotta R 2002 *International Journal of Thermal Sciences* **41** 217 – 227
[18] Dantas L, Orlande H and Cotta R 2003 *International Journal of Heat and Mass Transfer* **46** 1587 – 1598
[19] De Simon L, Iglesias M, Jones B and Wood C 2018 *Energy and Buildings* **177** 220 – 245 ISSN 0378-7788
[20] Rodler A, Guernouti S and Musy M 2019 *Construction and Building Materials* **196** 574 – 593 ISSN 0950-0618 URL `http://www.sciencedirect.com/science/article/pii/S0950061818327946`
[21] Incropera F, DeWitt D, Bergman T and Lavine A 2006 *Fundamentals of Heat and Mass Transfer* 6th ed (John Wiley and Sons, England) ISBN 9780471457282
[22] Trabelsi A, Slimani Z and Virgone J 2018 *International Journal of Heat and Mass Transfer* **127** 623–630
[23] Berger J, Gasparin S, Dutykh D and Mendes N 2020 *Building Simulation* **13** 1–18
[24] Gasparin S, Berger J, Dutykh D and Mendes N 2018 *Journal of Building Performance Simulation* **11** 129–144
[25] Crawley D B, Lawrie L K, Pedersen C O and Winkelmann F C 2000 *ASHRAE journal* **42** 49–56
[26] de la République Française J O 2010 Arrêté du 26 octobre 2010 relatif aux caractéristiques thermiques et aux exigences de performance énergétique des bâtiments nouveaux et des parties nouvelles de bâtiments
[27] Jumabekova A, Berger J, Foucquier A and Dulikravich G S 2020 *International Journal of Heat and Mass Transfer* **155** 119810 ISSN 0017-9310
[28] Berger J and Kadoch B 2020 *Building and Environment* **185** 107065